Scientia Iranica, Vol. 14, No. 1, pp 33–45

SCIENTIA IRANICA

Impedance Control of a Flexible Link Robot for Constrained and Unconstrained Maneuvers Using Sliding Mode Control (SMC) Method

G.R. Vossoughi* and A. Karimzadeh[1]

In this paper, the modeling and impedance-control of a one link flexible robot is presented. The concept of impedance control of flexible link robots is rather new and is being addressed for the first time. The control algorithm is valid for both constrained and unconstrained maneuvers. First, equations of motion and the associated boundary conditions are derived using Hamilton's principle. A linear finite dimensional model is, then, generated in the Cartesian coordinates, using the assumed mode method and by introduction of a proper coordinate transformation. The target impedance is, then, introduced in the Cartesian coordinate system and a control law is designed to realize the proposed target impedance for a given frequency range, using the Sliding Mode Control Theory. A set of computer simulations are carried out to demonstrate the effectiveness of the proposed control law. Simulations are carried out with various contact stiffness. As the results show, when the environmental surface stiffness is smaller than, or comparable to, that of the link, the control system is able to achieve stable behavior and the link vibration diminishes rather rapidly. However, when the environmental stiffness is much greater than that of the stiffness of the link, although the robot achieves stable behavior during contact, the vibrations tend to increase.

INTRODUCTION

The closed-loop motion control systems fall, in general, into two different classes: unconstrained and constrained systems. In the first case, the dynamic system (e.g., a manipulator) is driven in its workspace without contact with the environment. In the second case, the system is driven in its workspace in such a way that the environment continuously exerts a dynamic or kinematic constraint on the system's motion. A dynamic maneuver, such as leading a manipulator in a free environment towards a metal surface and, then, machine the surface, may consist of both types of maneuver.

The rejection of external forces is an important design specification when the dynamic system is unconstrained. Once the system crosses the boundary of the unconstrained environment (i.e., the dynamic system interacts with the environment), the dynamics of the system will change and stability will no longer be guaranteed with the same controller. In constrained maneuvering, the interaction load must be accommodated rather than resisted. If one defines "compliancy" as a measure of the stability of a dynamic system to react to interaction forces and torques, one can state the objective as assuring compliant motion in the global Cartesian coordinate frame for dynamic systems that must maneuver in a constrained condition.

Three general approaches to the compliant motion control include: Impedance control, stiffness control and hybrid position/force control. Hogan [1] first presented the idea of impedance control. In this method, neither the position nor the forces are controlled. In impedance control, one rather dictates a predefined dynamic – often second-order and referred to as the target impedance - between the motion (position and orientation) and the interaction loads (forces and torques). An impedance control system reduces to a

*. *Corresponding Author, Department of Mechanical Engineering, Sharif University of Technology, Tehran, I.R. Iran.*

1. *Department of Mechanical Engineering, Civil Aviation Technology College, Tehran, I.R. Iran.*

position control system during unconstrained maneuvers (because there are no interaction forces) and accommodates/controls contact forces during constrained conditions. Indeed, position control and force control are two extremes of impedance control. The former implies very high impedance, while the latter implies very low impedance.

Impedance control of rigid manipulators has been extensively addressed in the literature [1-6]. Many researchers have also considered the position, force and hybrid position/force control of flexible manipulators [7-15]. However, the problem of impedance control of a flexible manipulator has not yet been addressed in the literature. Impedance control provides a universal approach to the control of flexible robots - in both constrained and unconstrained maneuvers. This also allows for controlling the compliance of flexible robots/ structures beyond their natural compliance, making them more flexible or rigid, as needed.

In this article, a novel impedance-control strategy is presented for a one-link flexible manipulator using the Sliding Mode Control (SMC) theory. By including a term for the desired interaction force, the target impedance specification allows for force tracking during constrained maneuvers. Based on the SMC and eigenvalue assignment method, the dynamic system is forced in the sliding mode to achieve the desired impedance. Simulation results of the flexible link, during the transition from an unconstrained to constrained condition (wall with specified stiffness), are presented to demonstrate the effectiveness of the proposed impedance-control strategy.

MODELING

In this section, the modeling of a one degree of freedom flexible robot is carried out for use under two conditions: Unconstrained and constrained state. In the first case, it is assumed that the robot can move freely in its workspace without coming into contact with the environment. In the second case, it is assumed that the robot is in contact with an environment having a stiffness, k_e.

Modeling of an Unconstrained One-Link Flexible Robot

Let one consider a one-link flexible robot with length, l, mass per unit length, ρ, and uniform flexible rigidity, EI, that is driven by a motor in the horizontal plane by a torque, τ. The beam is assumed to be clamped on the motor's shaft with moment of inertia, J, and having a tip point mass, M, at the end. Let θ be the angle of rotation of the rotor and oxy representing the moving coordinate system, fixed to the rotor and rotating with angular velocity $\theta,(t)$ and angular acceleration, $\ddot{\theta}$,

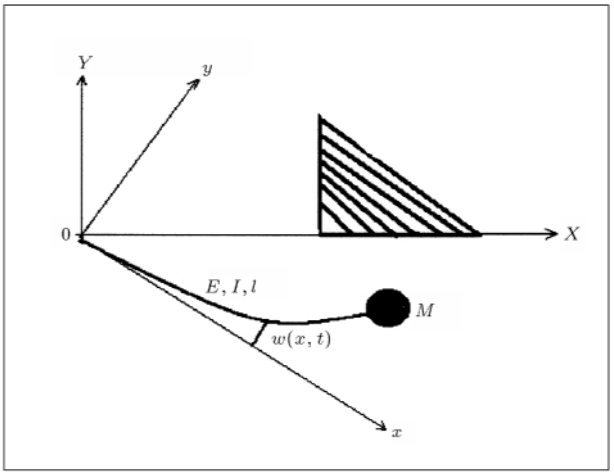

Figure 1. One-link flexible robot during an unconstrained maneuver (with point mass M).

about the inertial coordinate system, OXY. Referring to Figure 1, let $W(x,t)$ denote the deformation of any point, x, and $W_e(t) = W(l,t)$ be the end deflection of the beam at any time, t. To write equations of motion, the following assumptions are made:

- The effects of nonlinear terms $(W\dot{\theta})^2$ are small and negligible;
- The joint angle $\theta(t)$ is assumed to be small (i.e., $\sin(\theta) \approx \theta$, $\cos(\theta) = 1$);
- The rotational effects and shear deformations are negligible and the link is modeled as an Euler-Bernoulli beam.

Given the above assumptions, for any given point along the beam, one may write:

$$y(x,t) = x\theta \quad w(x,t). \tag{1}$$

The total kinetic and potential energies and the virtual work done by the motor are, then, given by:

$$E_k = \frac{1}{2}J\dot{\theta}^2 + \frac{\rho}{2}\int_0^l \dot{y}(x,t)^2 dx + \frac{1}{2}M\dot{y}(l,t)^2,$$

$$E_p = \frac{EI}{2}\int_0^1 y''(x,t)^2 dx,$$

$$\delta W = \tau\delta\theta. \tag{2}$$

Using Hamilton's principal yields:

$$\int_{t_0}^{t} (\delta E_k \quad \delta E_p + \delta W)dt = 0. \tag{3}$$

By separately calculating the variation of the parameter in Equation 3, one gets:

$$\delta E_k = J\dot{\theta}\delta\dot{\theta} + \rho\int_0^l (\dot{y}\delta\dot{y})dx + M\dot{y}(l,t)\delta\dot{y}(l,t),$$

$$\delta E_p = EI\int_0^l (y''\delta y'')dx. \tag{4}$$

Substituting Equation 4 into Equation 3 and using the integration by parts gives:

$$\delta\theta: \quad J\ddot{\theta} \quad \rho\int_0^l x\ddot{y}(x,t)dx \quad Ml\ddot{y}(l,t) + \tau(t) = 0, \tag{5}$$

$$\delta w: \ \rho\ddot{y}(x,t) + EIy''''(x,t) = 0, \tag{6}$$

$$\delta y(l,t): \quad M\ddot{y}(l,t) + EIy'''(l,t) = 0. \tag{7}$$

In obtaining the above equations, the following boundary conditions have been used:

$$w(0,t) = w'(0,t) = w''(l,t) = 0. \tag{8}$$

By substituting Equation 6 into Equations 5 and 7, one gets:

$$J\ddot{\theta} \quad EIy''(0,t) = \tau(t), \tag{9}$$

$$\rho\ddot{y}(x,t) + EIy''''(x,t) = 0. \tag{10}$$

The boundary conditions for Equation 10 are stated as:

$$y(0,t) = y''(l,t) = 0, \qquad y'(0,t) = \theta(t),$$

$$\frac{M}{\rho}y''''(l,t) + y'''(l,t) = 0. \tag{11}$$

By substituting Equation 1 into Equations 9 and 10, one obtains the equations of motion in the following forms:

$$j\ddot{\theta} + EIw''(0,t) = \tau(t), \tag{12}$$

$$\rho\ddot{w}(x,t) + EIw''''(x,t) = x\ddot{\theta}, \tag{13}$$

with the boundary conditions:

$$w(0,t) = w'(0,t) = w''(l,t) = 0, \tag{14}$$

$$Mw''''(l,t) + \rho w'''(l,t) = 0. \tag{15}$$

The above boundary Conditions are homogeneous, making the derivation of the finite dimensional modal model relatively straightforward using the assumed mode method.

Modeling of a Constrained One-Link Flexible Robot

One now proceeds to model a one-link flexible robot with its end-point in contact with an environment. As shown in Figure 2, it is assumed that the robot encounters a wall with a known stiffness exerting a force, $f(t)$, at the end-point of the robot.

The kinetic and potential energy of the link and the virtual work done by the motor may be written as:

$$E_k = \frac{1}{2}J\dot{\theta}^2 + \frac{\rho}{2}\int_0^l \dot{y}(x,t)^2dx + \frac{1}{2}M\dot{y}(l,t)^2,$$

$$E_p = \frac{EI}{2}\int_0^l y''(x,t)^2 + f(t)y(l,t),$$

$$\delta W = \tau\delta\theta. \tag{16}$$

Substituting Equation 16 into Equation 3 and integrating by parts yields:

$$J\ddot{\theta} \quad \rho\int_0^l x\ddot{y}(x,t)dx \quad Ml\ddot{y}(l,t) + \tau(t) \quad f(t)l = 0, \tag{17}$$

$$\rho\ddot{y}(x,t) + EIy''''(x,t) = 0, \tag{18}$$

$$EI(M\ddot{y}(l,t) + \rho y'''(l,t)) + \rho f(t) = 0. \tag{19}$$

Equations 17 and 18 describe the equation of motion for the flexible link. Equation 19 gives a boundary condition at $x = l$. The other three B.C's for Equation 18 are, as follows:

$$y(0,t) = y''(l,t) = 0, \qquad y'(0,t) = \theta(t). \tag{20}$$

Substituting Equation 18 into Equations 19 and 17, one

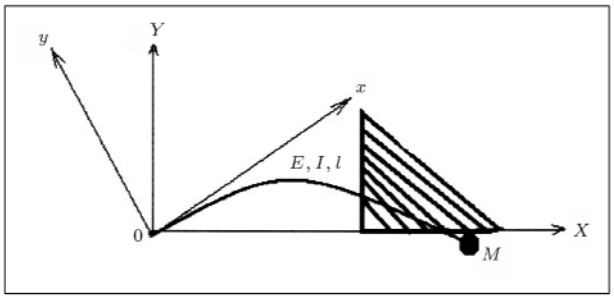

Figure 2. Constrained one-link flexible robot in contact with environment (with known stiffness K_e).

obtains:

$$J\ddot{\theta} \quad EIy''(0,t) = \tau(t), \tag{21}$$

$$\rho\ddot{y}(x,t) + EIy''''(x,t) = 0, \tag{22}$$

$$y(0,t) = y''(l,t) = 0, \tag{23}$$

$$y'(0,t) = \theta(t), \tag{24}$$

$$EI\left(\frac{M}{\rho}y''''(l,t) + y'''(l,t)\right) = \quad f(t). \tag{25}$$

Substituting Equation 1 into Equations 21 to 25 gives:

$$j\ddot{\theta} + EIw''(0,t) = \tau(t), \tag{26}$$

$$\rho\ddot{w}(x,t) + EIw''''(x,t) = x\ddot{\theta}, \tag{27}$$

$$w(0,t) = w'(0,t) = w''(l,t) = 0, \tag{28}$$

$$EI\left(\frac{M}{\rho}w''''(l,t) + w'''(l,t)\right) = f(t). \tag{29}$$

Note that the boundary condition in Equation 29 is non-homogenous, calling for special attention. In the following section, a finite dimensional modal model will be derived for the robot in both unconstrained and constrained conditions, one that is suitable for the controller design applications.

CONSTRUCTION OF FINITE DIMENSIONAL MODEL

A finite dimensional model is constructed for both unconstrained and constrained cases. In order to construct a finite dimensional model, the eigen-function expansion method is used.

Unconstrained-Case

Substituting $w(x,t) = \sum_{i=1}^{N} \varphi_i(x)q_i(t)$ into Equations 12 and 13 and multiplying every term by $\varphi_i(x)$, one obtains:

$$\ddot{q}_i(t) = \quad \omega_i^2 q_i(t) + b_i\ddot{\theta} \quad \delta\omega_i^2\dot{q}_i(t), \tag{30}$$

$$J\ddot{\theta} + EI\sum_{i=1}^{N}\varphi_i''(0)q_i(t) = \tau(t). \tag{31}$$

In which, $\varphi_i(x)$ represents the solution of the Euler-Bernoulli beam (with the given boundary conditions), and ω_i and δ are the frequency of vibrations and the small structural viscous damping of the beam's material, respectively. Other parameters are defined as:

$$b_i = < x, \varphi_i(x) >, \tag{32}$$

$$< \varphi_i, \varphi_j > = \int_0^l \varphi_i\varphi_j dx + \frac{M}{\rho}\varphi_i(l)\varphi_j(l),$$

$$< \varphi_i, \varphi_j > = 0 \quad \text{if } i \neq j. \tag{33}$$

Constrained-Case

Substituting $w(x,t) = \sum_{i=1}^{N} \varphi_i(x)q_i(t)$ into Equations 26 and 27 and multiplying both sides by $\varphi_i(x)$, results in:

$$\ddot{q}_i(t) = \quad \omega_i^2 q_i(t) + b_i\ddot{\theta} \quad \delta\omega_i^2\dot{q}_i(t) \quad (\varphi_i(l)/\rho)f(t), \tag{34}$$

$$J\ddot{\theta} + EI\sum_{i=1}^{N}\varphi_i''(0)q_i(t) = \tau(t), \tag{35}$$

$$b_i = < x, \varphi_i(x) >, \tag{36}$$

where $\varphi_i(x)$ is the solution of the following equation and boundary conditions:

$$\varphi'''' = (\rho\omega^2/EI)\varphi, \tag{37}$$

$$\varphi(0) = \varphi'(0) = \varphi''(l) = 0, \tag{38}$$

$$M\varphi''''(l) + \rho\varphi'''(l) = 0, \tag{39}$$

and ω is the frequency of vibrations.

MODELING IN THE CARTESIAN COORDINATE SYSTEM

Since the target impedance is always defined in the Cartesian coordinate system, the dynamic model shall be expressed in the Cartesian coordinate system. One can use Equations 1 to construct a transformation between end point coordinate $x(t)$ and the joint coordinate $\theta(t)$:

$$x(t) = l\theta \quad \sum_{i=1}^{n} q_i(t)\varphi_i(l). \tag{40}$$

Differentiating Equation 40 and using Equation 34, one gets:

$$\ddot{x} = k_t u(t) + \sum_{i=1}^{n} k_i q_i(t) + c_i\dot{q}_i(t) + af(t), \tag{41}$$

where:

$$k_t = l \quad \sum_{i=1}^{n} b_i \varphi_i(l), \quad k_i = \varphi_i(l)\omega_i^2,$$

$$c_i = \delta k_i, \quad a = \sum_{i=1}^{n} \varphi_i(l)^2/\rho, \tag{42}$$

and $u(t) = \ddot{\theta}(t)$ is considered as the control input. In Equation 34 and Equation 41, when the robot moves freely without any environmental contact, then, $f(t) = 0$ and, as long as the endpoint is in contact with the environment, one has $f(t) = \quad k_e x(t)$, where k_e is environmental stiffness at the point of contact.

Equations 34 and 41 can be written in the state space form, as follows:

$$\dot{X} = AX + Bu + B_f f(t), \tag{43}$$

where:

$$A = \begin{bmatrix} A_{11} & A_{12} \\ A_{21} & A_{22} \end{bmatrix},$$

$$A_{22} = \begin{bmatrix} 0 & 1 & 0 & 0 & \cdots & \cdots & 0 \\ \omega_1^2 & \delta\omega_1^2 & 0 & 0 & \cdots & \cdots & 0 \\ 0 & 0 & 0 & 1 & 0 & \cdots & 0 \\ 0 & 0 & \omega_2^2 & \delta\omega_2^2 & 0 & \cdots & 0 \end{bmatrix},$$

$$s_i = \quad \frac{\varphi_i(l)}{\rho},$$

$$A_{12} = \begin{bmatrix} 0 & 0 & 0 & 0 & 0 & 0 \\ k_1 & c_1 & \cdots & \cdots & k_n & c_n \end{bmatrix}_{2\times 2n},$$

$$B_2 = \begin{bmatrix} 0 & b_1 & 0 & b_2 & \cdots \end{bmatrix}^T_{2n\times 1},$$

$$A_{11} = \begin{bmatrix} 0 & 0 \\ 0 & 1 \end{bmatrix}_{2\times 2},$$

$$B_f = \begin{bmatrix} 0 & a & 0 & s_1 & 0 & s_2 & \cdots \end{bmatrix}^T_{(2n+2)\times 1},$$

$$B = \begin{bmatrix} B_1 \\ B_2 \end{bmatrix},$$

$$A_{21} = [0]_{2n\times 2},$$

$$B_1 = \begin{bmatrix} 0 \\ k_t \end{bmatrix}_{2\times 1}. \tag{44}$$

DESIGN OF A SLIDING MODE CONTROLLER FOR ACHIEVING TARGET IMPEDANCE

In this section, a control system is designed to achieve the desired target impedance. The controller enables one to control the behavior of the robot in the constrained as well as unconstrained condition. In the unconstrained case, in effect, the position will be controlled and in the constrained condition, a dynamic relationship between position error and contact force is controlled.

The target impedance is, usually, of the second order nature and is given by [4,5]:

$$M\ddot{e} + C\dot{e} + Ke = \quad f(t),$$

$$e = x(t) \quad x_d, \tag{45}$$

where x_d and $f(t)$ are the desired end-point position and contact force respectively. In a multi-input multi-output case, M, C and K are positive definite matrices. In the next section, the role and the selection guidelines for each of the three parameters M, C and K will be discussed.

DESIGN OF THE SLIDING SURFACE

In the previous section, the dynamics of the system were presented in state space form. Assuming that matrix B has full rank m (m is the number of inputs), there exists an orthogonal $(2n+2)\times(2n+2)$ transformation matrix, T, such that:

$$TB = \begin{bmatrix} 0 \\ B_2 \end{bmatrix}, \tag{46}$$

where B_2 is $m \times m$ and a nonsingular matrix. The orthogonality restriction is on T, for reason of numerical stability and to remove the problem of inverting T when transforming back to the original system. A suitable method for determining T is the QU factorization, where B is decomposed into the form:

$$B = Q \begin{bmatrix} U \\ 0 \end{bmatrix}. \tag{47}$$

With Q $n \times n$ and orthogonal, and U $m \times m$, nonsingular and upper triangular, T is, then, determined by rearranging the rows of Q^T.

By writing Equation 43 in terms of the transformed state variable, $y = TX$, one has:

$$\dot{y}(t) = (TAT^T)y(t) + (TB)u + (TB_f)f(t). \tag{48}$$

The transformed state, Y, and the state Equation 48 may be now partitioned as:

$$y^T = [y_1^T,\ y_2^T],$$

$$y_1 \in R^{n\quad m},$$

$$y_2 \in R^m, \tag{49}$$

and the matrices TAT^T, TB and TB_f are partitioned accordingly, then, Equation 48 may be written in the form:

$$\dot{y}_1 = \overline{A}_{11}y_1 + \overline{A}_{12}y_2 + \overline{B}_{f1}f(t), \tag{50}$$

$$\dot{y}_2 = \overline{A}_{21}y_1 + \overline{A}_{22}y_2 + B_2u + \overline{B}_{f2}f(t), \tag{51}$$

$$TAT^T = \begin{bmatrix} \overline{A}_{11} & \overline{A}_{12} \\ \overline{A}_{21} & \overline{A}_{22} \end{bmatrix}. \tag{52}$$

Now, if one defines the sliding surface as:

$$s = CX = 0. \tag{53}$$

The main goal will be the determination of elements of matrix C, so that the desired target impedance is obtained in the sliding mode.

The sliding surface, in terms of the transformed state, y, can be stated as:

$$s=(CT^T)y=\begin{bmatrix}\overline{C}_1 & \overline{C}_2\end{bmatrix}\begin{bmatrix}y_1 & y_2\end{bmatrix}^T=\overline{C}_1y_1+\overline{C}_2y_2=0. \tag{54}$$

Condition 54, defining the sliding mode, may now be written as:

$$y_2(t) = \quad Fy_1(t), \tag{55}$$

where the $m \times (2n+2 \quad m)$ matrix, F, is defined by:

$$F = \overline{C}_2{}^{1}\overline{C}_1. \tag{56}$$

This indicates that the evolution of y_2 in the sliding mode is related linearly to that of y_1. The ideal sliding mode is, therefore, governed by the following equations:

$$\dot{y}_1 = \overline{A}_{11}y_1 + \overline{A}_{12}y_2 + \overline{B}_{f1}f(t), \tag{57}$$

$$y_2(t) = \quad Fy_1(t), \tag{58}$$

which is an $(2n+2 \quad m)$th order system, in which y_2 plays the role of a state feedback controller. Substituting Equation 58 into Equation 57 results in the following closed loop dynamic:

$$\dot{y}_1 = \quad \overline{A}_{11} \quad \overline{A}_{12}F\big)\, y_1 + \overline{B}_{f1}f(t), \tag{59}$$

which indicates that the design of stable sliding mode dynamics ($y_1 \to 0$ as $t \to \infty$) requires the determination of the gain matrix, F, such that $\overline{A}_{11} \quad \overline{A}_{12}F$ has $(2n+2 \quad m)$ left hand half-plane eigenvalues. This may be achieved using a conventional pole-placement method, i.e., one that minimizes an integral square cost function. Here, one can use the pole placement method to place the eigenvalues of Equation 59 in the desired locations. However, to achieve the target impedance Equation 45, one must choose the feedback gain, F, such that eigenvalues of Equations 59 and 45 are equal. In a multi-input case, one has to use the eigenstructure assignment method to match the dynamics of Equations 59 and 45. A problem which arises in a flexible robot is that of the order of the dynamics in Equation 59 being much higher than that of Equation 45, depending upon the number of the assumed modes in the model. Hence, the eigenvalue assignment is nontrivial. This problem will be considered, in detail, in the next section.

It is noted that whichever scheme one chooses for the design, fixing F does not uniquely determine C. This is due to the $F = \overline{C}_2{}^{1}\overline{C}_1$ degrees of freedom in the following relationship:

$$\overline{C}_2F = \overline{C}_1. \tag{60}$$

A simple method of determining C, is to let $\overline{C}_2 = I_m$ (identity matrix). This gives:

$$C = \begin{bmatrix} F & I_{m\times m}\end{bmatrix} T. \tag{61}$$

This approach has the merit of minimizing the amount of calculations and, hence, reducing the possibility of numerical error.

SLIDING MODE CONTROLLER DESIGN

Now, one is ready to design a control law for achieving the desired impedance in Equation 45, i.e., bringing the systems state variables onto the sliding surface at a finite time and maintaining the state trajectory on the surface. Various methods are proposed for reaching the sliding surface. A simple reaching law, proposed by Slotine [16-18], is as follows:

$$\dot{s}(t) = \quad k\,\mathrm{sgn}(s) \quad \alpha s(t) \quad \beta\int_0^t s(t)dt, \tag{62}$$

where α, β and k are positive numbers. The sgn(s) is defined by:

$$\mathrm{sgn}(s) = \begin{cases} 1 & s > 0 \\ 0 & s = 0 \\ 1 & s < 0 \end{cases}. \tag{63}$$

By differentiating Equation 54 and substituting from Equations 62 and 43, one can obtain the following

control input:

$$u = \quad (CB) \quad ^{1}\{CAX + CB_f f(t) + F(s)\}, \tag{64}$$

$$F(s) = k\,\mathrm{sgn}(s) + \alpha s(t) + \beta \int s(t)dt, \tag{65}$$

in which $\det(CB) \neq 0$ is the necessary condition for controllability. The control law in Equation 64 guarantees that the system reaches the sliding surface at a finite time and stays on the sliding surface thereafter. Once the sliding mode initiates, the dynamics in Equation 59 are realized and the desired impedance is achieved. The discontinuous function, sgn, in the control law Equation 64 causes high frequency chattering in the sliding mode, which is undesirable. To overcome this problem, the sgn(.) function is replaced with the piecewise continuous function, sat(.):

$$\mathrm{sat}(s/\phi) = \begin{cases} 1 & s > \varphi \\ s/\varphi & |s| < \varphi \\ 1 & s < \quad \varphi \end{cases}, \tag{66}$$

in which, ϕ is a positive number, known as the boundary layer. This parameter must be chosen as small as possible to eliminate the chattering.

SELECTION OF THE TARGET IMPEDANCE

In the previous section, the desired impedance was defined as:

$$M\ddot{e} + C\dot{e} + Ke = \quad f(t), \qquad 0 < \omega < \omega_0, \tag{67}$$

in which $(0, \omega_0)$ is the frequency interval at which one wants to realize the desired impedance. One usually selects the K matrix to limit the desired interaction forces and torques. The choices of inertia matrix (M) and damping matrix C assure the achievement of ω_0 and stability of the system.

A small ω_0 will also allow one to meet strong sets of stability robustness specifications at high frequencies. On the other hand, with a very small ω_0, stability robustness to parameter uncertainties may not be satisfied. This is true because stability robustness to parameter uncertainties assign a lower bond on ω_0. To achieve a wide ω_0, one should have a good model of the system at high frequencies (and, consequently, a weak set of stability robustness specifications at high frequencies).

Because of the conflict between the desired ω_0 and stability robustness to high frequency un-modeled dynamics, it is a struggle to meet both sets of specifications for a given model of uncertainty. The frequency range of operation, ω_0, cannot be selected to be of an arbitrary wide, if a good model of the system does not exist at high frequencies, while a good model of the system at high frequencies makes it possible to retain the target dynamics for a wider range of frequencies $(0, \omega_0)$.

EIGENVALUES ASSIGNMENT OF THE VIBRATION MODES

One of the main issues in the impedance control of flexible link robots is that the number of eigenvalues of the target impedance is much smaller than the number of modes of the system. To overcome this, one must place the eigenvalues associated with the vibration modes far from the origin, relative to the eigenvalues of the target impedance. This makes the dynamics of the target impedance dominant.

Letting ω_i and $\xi_i (i = 1 \cdots n)$ be the frequency and damping coefficient of the ith vibration mode, the eigenvalues are placed at $\alpha\omega_i\xi_i \pm \omega_j$, where α is a positive number that must be properly selected. In selecting α, the control system must preserve the stability robustness specification over the frequency range $(0, \omega_0)$. Proper selection of α requires experience and understanding of the system. α must be large enough to guarantee that the performance specification will be met, but also, small enough to fulfill the stability robustness specification. Because one needs to have a relatively large α (because ξ_i's are very small), one has to choose the frequency range, ω_0, as small as possible.

BEHAVIOR OF IMPEDANCE CONTROL IN UNCONSTRAINED AND CONSTRAINED CONDITIONS

If, for a robot manipulator, the impedance in Equation 45 is realized over a specified frequency range $(0, \omega_0)$, depending upon the environment with which the robot interacts, one can consider two modes for impedance control. These modes are position control and regulating force control.

Unconstrained Case

Before any contact (and in the absence of any contact force $f(t) : f(t) = 0$), the arm is actually under position control. In this phase, the governing impedance equation is:

$$M\ddot{e} + C\dot{e} + Ke = \quad f(t) = 0, \qquad e = x \quad x_d.$$

Thus, if the target impedance in Equation 45 is stable (by proper selection of parameters M, C and K), then, the error $e = x \quad x_d$ is guaranteed to approach zero, thereby, achieving position control $(x \to x_d)$.

Constrained Case

After contact (and in the presence of contact force $f(t)$) the arm is actually under endpoint "force compensation". In this phase, the governing impedance equation (assuming $x_e = 0$) is:

$$M\ddot{e} + C\dot{e} + Ke = f(t) = K_e(x)$$

$$\Rightarrow M\ddot{e} + C\dot{e} + (K + K_e)e$$

$$= K_e(x_d), \tag{68}$$

where $e = x \quad x_d$ and $K_e =$ environmental stiffness:

Steady state position error:

$$e = \frac{K_e}{(K + K_e)}(x_d)$$

$$x \rightarrow \left(\frac{K}{K + K_e}\right) x_d, \tag{69}$$

Steady state contact force:

$$f = K_e x = \frac{K K_e}{K + K_e} x_d,$$

$$f = \frac{K}{K + K_e} f_d. \tag{70}$$

If one assumes the desired contact force is modulated by the desired position, x_d, as in $f_d = k_e(x_d)$, then, one gets:

$$\text{Steady state contact force } f = K_e.x = \frac{K}{K + K_e} f_d. \tag{71}$$

Thus, under contact conditions, one can get controlled regulation of the contact forces by proper selection of the impedance parameter, K, or by location of the eigenvalues of the target impedance in Equation 45. Accurate control of the contact force requires the use of force error in the impedance control law and will not be pursued here.

COMPUTER SIMULATION RESULTS

The simulations are carried out to demonstrate the effectiveness of the proposed impedance control law. The simulation is done for two cases: (a) A wall stiffness, $K_e = 100$ (N/m) and (b) A wall stiffness, $K_e = 1000$ (N/m). Other assumed parameters are:

$l = 0.9$ (m), $E = 2.06e11$,
$I = 1.41e \quad 11$ (m^4), $\rho = 0.405$ (kg/m),
$\delta = 1.2e \quad 4$ (N.s/m), $M = 0.66$ (kg),
$J = 0.2$, $a = 1000$,
$b = 500$, $k = 0.2$,

$x_d = 0.08 + 0.05t$ (m) (for unconstrained case),

$x_d = 0.02$ (for constrained case).

The equivalent stiffness and mass at the end of the beam can be given by:

$$K_{eq} = \frac{3EI}{l^3} >> 12 \text{ [N/m]},$$

$$M_{eq} = \frac{\rho l}{3} = 0.12 \text{ [kg]}.$$

Impedance parameters for two cases are given as:

for unconstrained phase:

$M = 0.06,\ C = 2.1,\ K = 16,\ \omega_0 = 15(\text{rad/s}),\ \alpha = 50,$

for constrained phase:

$M = 0.06,\ C = 1.8,\ K = 12.5,\ \omega_0 = 15(\text{rad/s}),\ \alpha = 50,$

contact time:

$t = 1.6$[sec].

The simulation has been carried out using two modes for the controller design and using four modes for the model simulation. For each case, the first mode $q_1(t)$, second mode, $q_2(t)$, end point position, $y(t)$, joint angle, $\theta(t)$, angular velocity, $\dot{\theta}(t)$, and contact force, $f(t)$, are plotted. Figures 3 to 8 show the results for Case (a). As the results show, the link has a stable behavior before and during contact with the environment. Moreover, the vibration modes

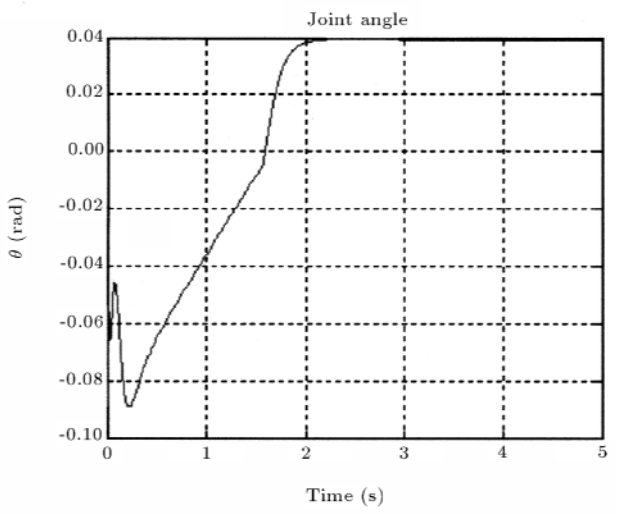

Figure 3. Transient response of θ for Case (a).

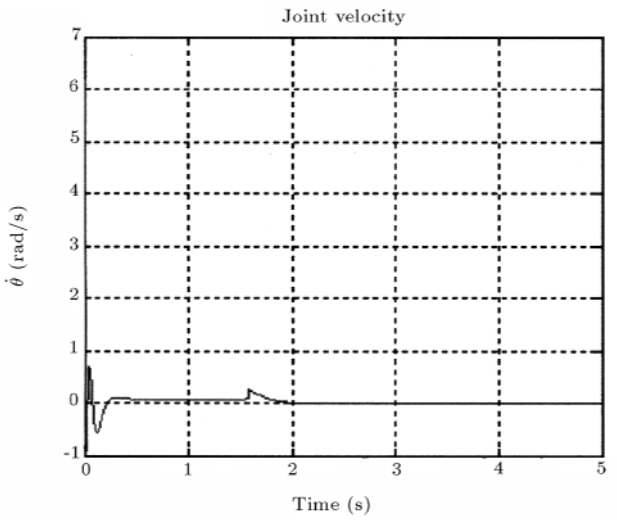

Figure 4. Transient response of $\dot{\theta}$ for Case (a).

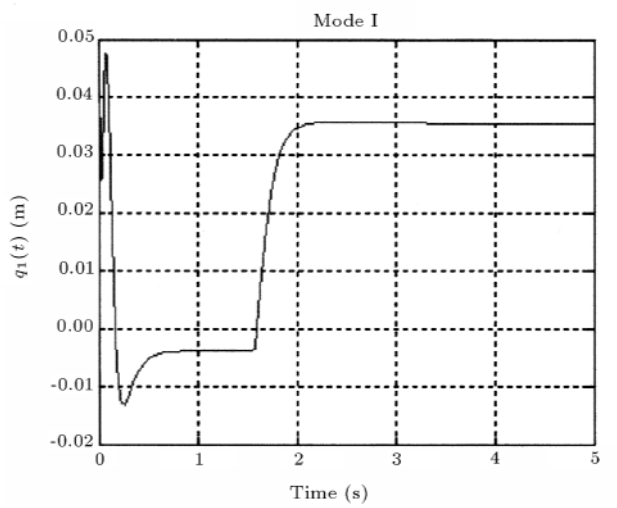

Figure 5. Transient response of vibration Mode I for Case (a).

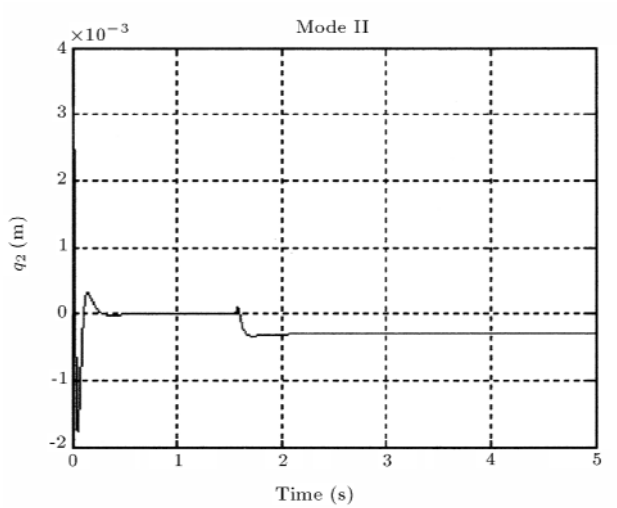

Figure 6. Transient response of vibration Mode II for Case (a).

have also been shown to die out after contact. As discussed previously, before the contact ($t < 1.6$), the impedance controller acts as a simple position controller and, during the contact ($t > 1.6$), as a regulating force controller. As shown in Figures 7 and 8, there are steady state errors in the contact force and endpoint position, according to Equations 69 and 70. Figures 9 to 14 represent the results for Case (b). In this case, the stiffness of the surface is much greater than that of the link. In this case, also, the link vibrations are damped out before and during the contact. In this case, separation did not occur, but, if the stiffness of the environment increases, separation may also occur during the contact. As shown in Figures 13 and 14, steady state position and contact force errors in this case are larger than that of Case (a). This increase in the steady state errors resulting from higher environmental stiffness is also predicted from

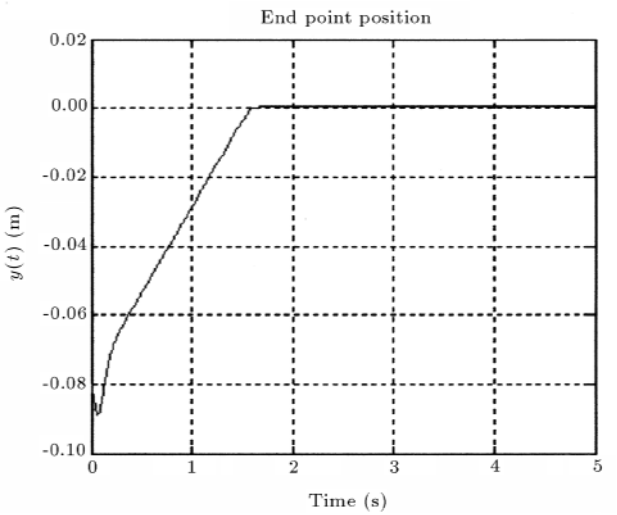

Figure 7. Transient response of $y(t)$ for Case (a).

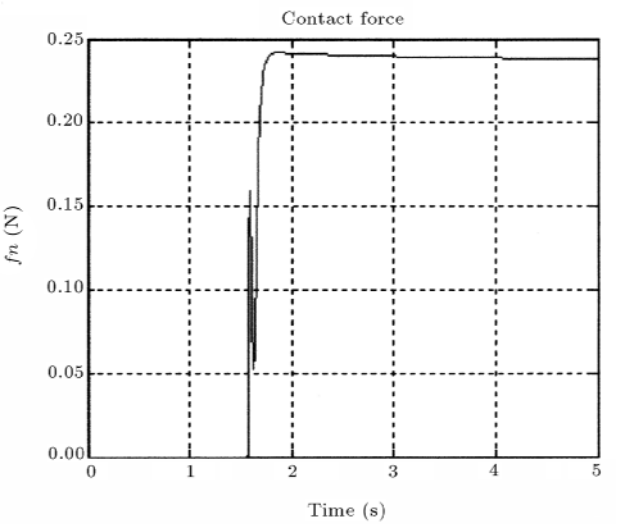

Figure 8. Transient response of $f_n(t)$ for Case (a).

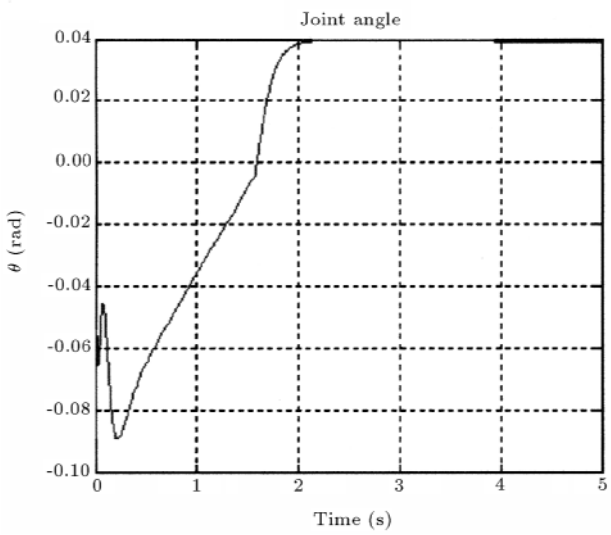

Figure 9. Transient response of θ for Case (b).

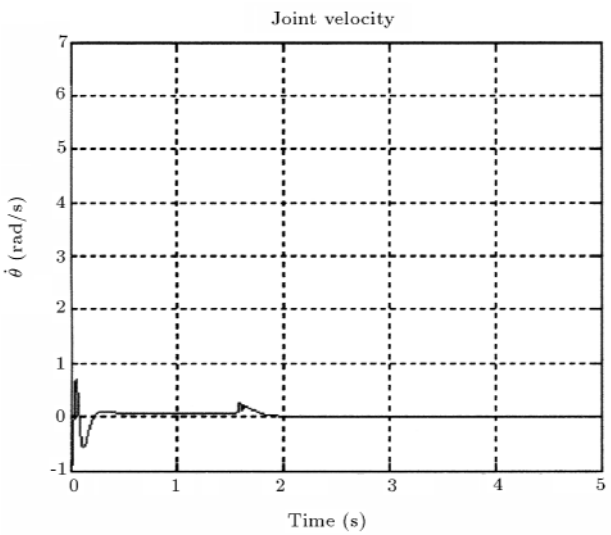

Figure 10. Transient response of $\dot{\theta}$ for Case (b).

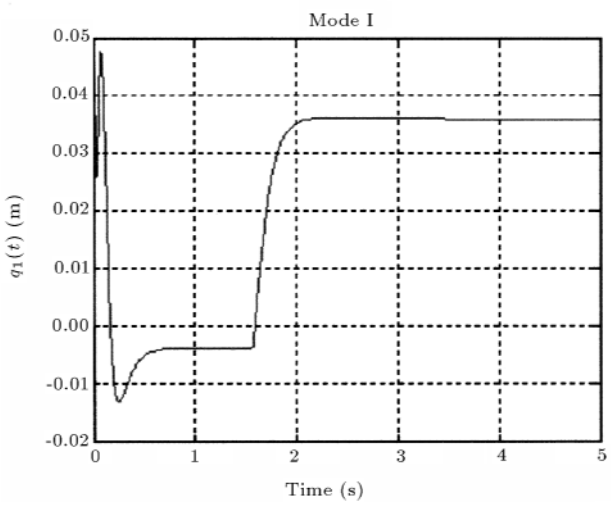

Figure 11. Transient response of vibration Mode I for Case (b).

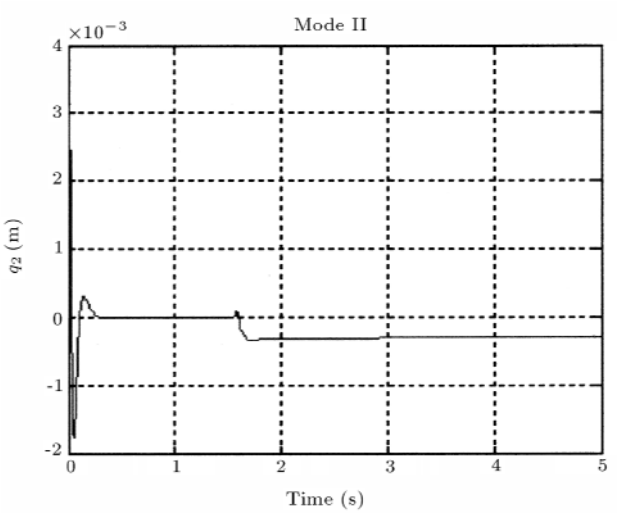

Figure 12. Transient response of vibration Mode II in Case (b).

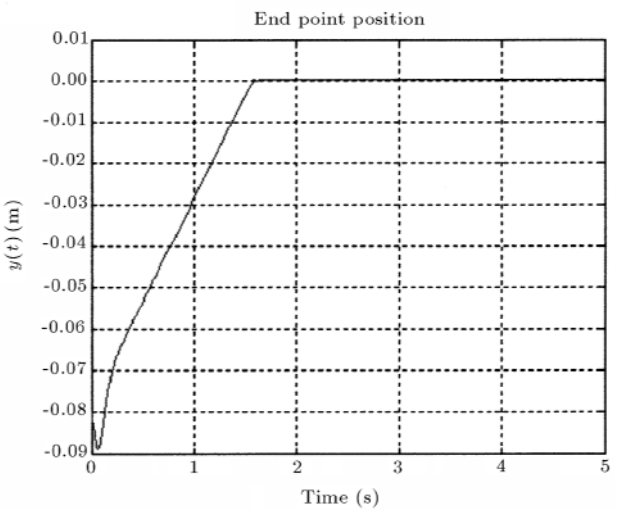

Figure 13. Transient response of $y(t)$ for Case (b).

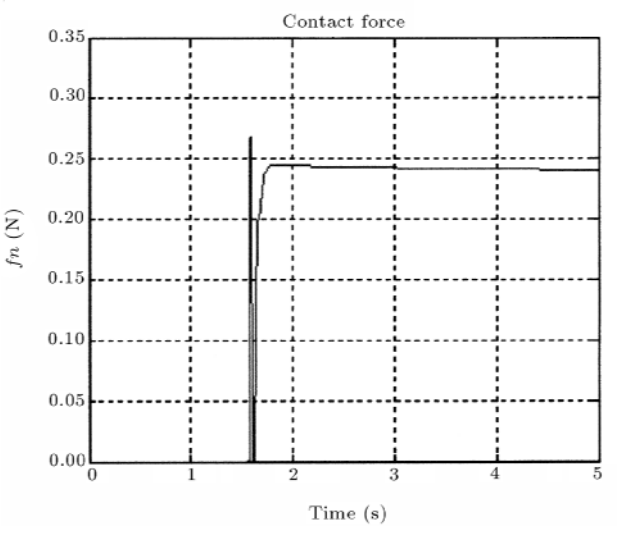

Figure 14. Transient response of $f_n(t)$ for Case (b).

Equations 69 and 70. One should also note that, as the eigenvalues for target impedance are moved further to the left (in the left half plane), the effective endpoint stiffness of the robot increases to values much larger than the inherent endpoint flexibility and instability during contact becomes inevitable. Simulation with eigenvalues, $\lambda < 20$, leads to unstable behavior during contact (results not shown here). A simulation was also carried out with two sets of eigenvalues that correspond to the value of $K = 8$ N/m and $K = 15$ N/m (different from the inherent endpoint stiffness $K_{eq} \approx 12$ N/m), in order to show the effects of parameter K on the impedance controller. These results are shown in Figures 15 to 20 and are labeled as Case (c).

Based on the above results, one can conclude that the proposed impedance control strategy has enabled one to control the behavior of the flexible link robot in

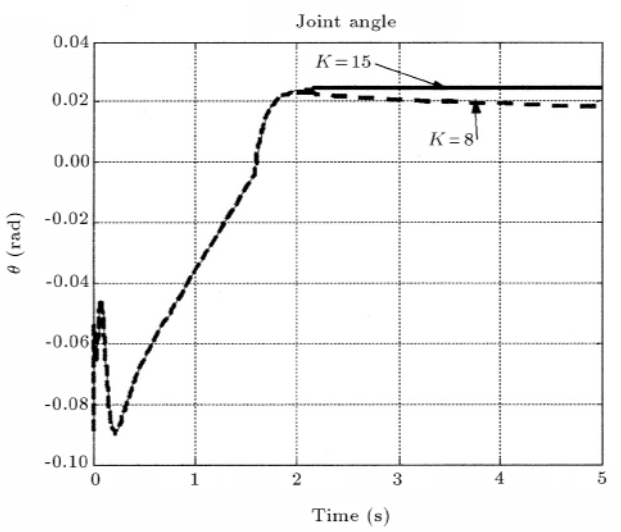

Figure 15. Transient response of θ for Case (c).

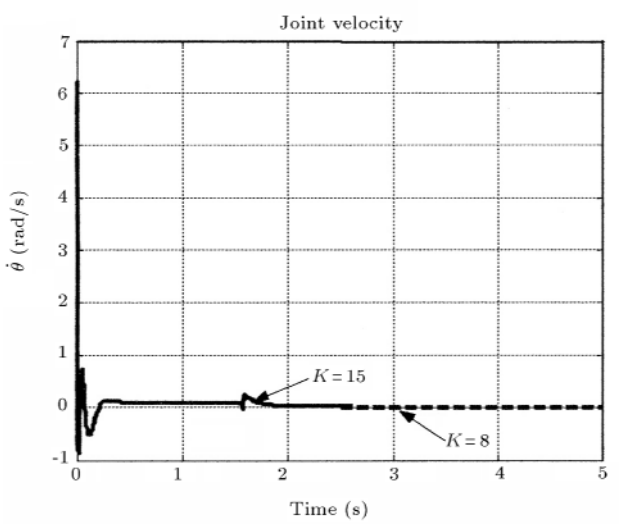

Figure 16. Transient response of $\dot{\theta}$ for Case (c).

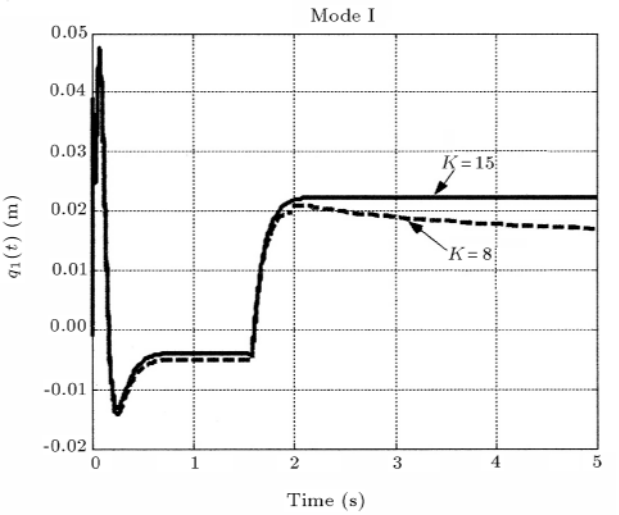

Figure 17. Transient response of Mode I for Case (c).

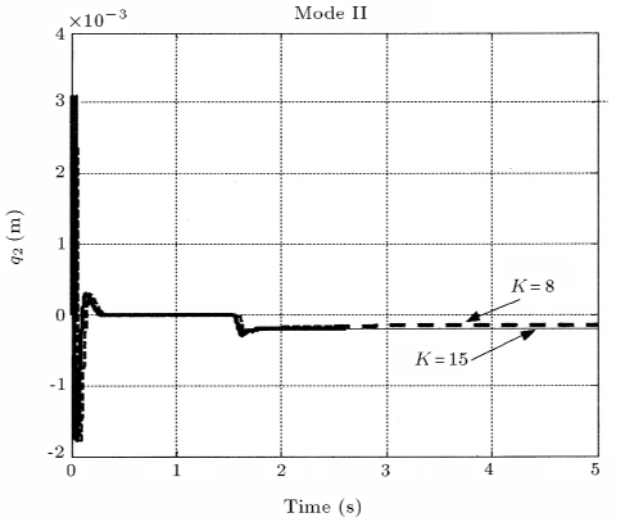

Figure 18. Transient response of Mode II for Case (c).

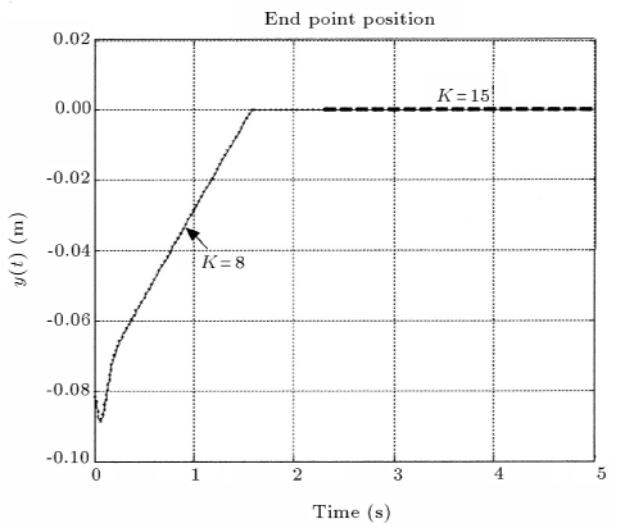

Figure 19. Transient response of $y(t)$ for Case (c).

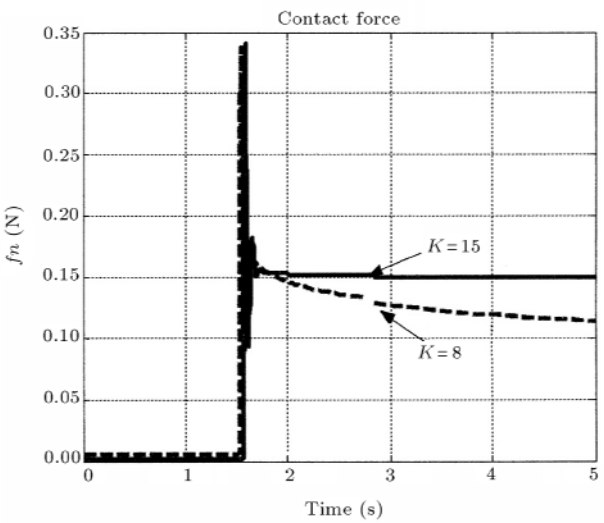

Figure 20. Transient response of $f_n(t)$ for Case (c).

both constrained and unconstrained conditions, a capability that would, otherwise, require two controllers, each with a different control structure.

CONCLUDING REMARKS

In this paper, the modeling and impedance control of a flexible link manipulator, using a sliding mode control technique, have been considered. The proposed controller works well in both unconstrained and constrained conditions. One can control the behavior of the manipulator, in both conditions, using a single controller with a single structure (by only tuning the impedance parameters). The use of the sliding mode control theory provides a suitable domain for future research into issues such as robustness and the effects of various nonlinear effects, actuator dynamics and other uncertainties and external disturbances. These studies should be complemented by experimental results to further validate the proposed control method.

NOMENCLATURE

k_e	stiffness of environment
L	length of robot
ρ	mass per unit length
EI	flexural rigidity of link
M	tip mass
θ	joint angle
$w(x,t)$	deflection of any point x at time t
$w_e(t) = w(l,t)$	end point deflection of link
E_k	kinetic energy
E_p	potential energy
δW	virtual work done of motor
J	moment inertia of rotor
$f(t)$	normal contact force
$\omega_i (i = 1...n)$	natural frequency of link
$\varphi_i(x)$	mode shape of link
δ	small structural damping of link
$\tau(t)$	torque developed by motor
$x(t)$	end point position
$x_d(t)$	desired motion trajectory
M	desired mass matrix
K	desired stiffness matrix
B	desired damping matrix
$u(t)$	control input
T	transformation matrix

REFERENCES

1. Hogan, N. "Impedance control: An approach to manipulation: Part I, Part II, Part III", *ASME J. Dynamic Syst. Measurement. Contr.*, **107**(1), pp 1-24 (1987).
2. Kelly, R. and Carelli, R. et al. "Adaptive impedance control of robot manipulators", *Int. J. Robotics and Automation*, **4**(3), pp 134-141 (1989).
3. Kosuge, K. and Yokoyama, T. "Mechanical impedance control of robot arm by virtual internal model following controller", *Proc. IFAC 10th Triennial World Congress*, Munich, Germany, **4**, pp 239-244 (1987).
4. Kazerooni, H. and Sheridan, T.B. et al. "Robust compliant motion for manipulators, Part I: The fundamental concept of compliant motion; Part II: Design method", *IEEE. J. Robotics and Automation*, **2**(2), pp 83-105 (1985).
5. Chan, S.P. and Gao, W.B. "Robust impedance control of robot manipulators", *Int. J. Robotic and Automation*, **6**(4), pp 220-227 (1991).
6. Purboghart, F. "Virtual adaptive compliant control for robots", *Int. J. Robotics and Automation*, **4**(3), pp 148-157 (1988).
7. Raibert, M.H. and Craig, J.J. "Hybrid position/force control of manipulators", *Trans. ASME J. Dyn. Sys. Meas. Control.*, **03**(2), pp 126-133 (1981).
8. Khatib, O. "A unified approach to motion and force control of robot manipulators: The operational space formulation", *IEEE Trans. Robotics Automation*, **RA-3**(1), pp 43-53 (1987).
9. Oshikawa, T. "Dynamic hybrid position/force control of robot manipulators-description of hand constraints and calculation of joint driving force", *IEEE Trans. Robotic Automation*, **RA-3**(5), pp 386-392 (1987).
10. McClamroch, N.H. and Wang, D. "Feedback stabilization and tracking of constrained robots", *IEEE Trans Automatic Control*, **Ac-33**(5), pp 419-426 (1988).
11. Fukada, T. "Flexibility control of elastic robotic arms", *J. Robotic Syst.*, **21**, pp 73-88 (1985).

12. Chiou, C. and Shahinpoor, M. "Dynamic stability analysis of two-link force-controlled flexible manipulator", *ASME J. Dyn. Sys. Meas. Control*, **112**(6), pp 661-666 (1990).

13. Matsuno, F. and Sakawa, Y. et al. "Quasi-static hybrid position/force control of a flexible manipulator", *Proc. IEEE Int. Conf on Robotics and Automation*, Sacramento, USA, pp 2838-2842 (1991).

14. Matsuno, F. and Asano, T. et al. "Quasi-static hybrid position/force control of two-degree-of-freedom flexible manipulators", *Proc. IEEE/RSJ Int. Workshop on Intelligent Robots and Systems'91 (IRSO'91)*, Osaka, Japan, pp 984-989 (1991).

15. Matsuno, F. and Yamamoto, K. "Dynamic hybrid position/force control of a two degree-of freedom flexible manipulator", *Journal of Robotic Systems*, **11**(5), pp 355-366 (1994).

16. Slotine, J.J. and Li, W., *Applied Nonlinear Control*, Prentice-Hall (1990).

17. Li, D. and Slotine, J.J. " On sliding control for multi-input multi-output nonlinear system", *Proc. American Control Conf.*, pp 874-79 (1987).

18. Slotine, J.J. "Sliding controller design for nonlinear systems", *Int. J. Control*, **40**(2), pp 101-109 (1994).